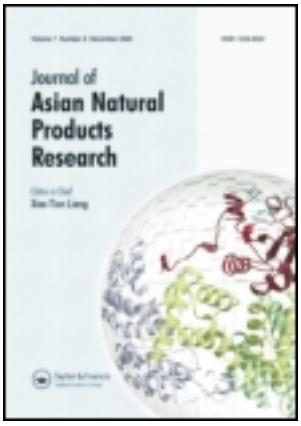

Journal of Asian Natural Products Research

Publication details, including instructions for authors and subscription information:
http://www.tandfonline.com/loi/ganp20

In-vitro antitumor activity evaluation of hyperforin derivatives

Feng Sun [a], Jin-Yun Liu [a], Feng He [a], Zhong Liu [b], Rui Wang [b], Dong-Mei Wang [a], Yi-Fei Wang [b] & De-Po Yang [a]

[a] School of Pharmaceutical Sciences, Sun Yat-Sen University, Guangzhou, 510006, China

[b] Biomedicine Research and Development Center, Jinan University, Guangzhou, 510632, China

Available online: 13 Jul 2011

To cite this article: Feng Sun, Jin-Yun Liu, Feng He, Zhong Liu, Rui Wang, Dong-Mei Wang, Yi-Fei Wang & De-Po Yang (2011): *In-vitro* antitumor activity evaluation of hyperforin derivatives, Journal of Asian Natural Products Research, 13:8, 688-699

To link to this article: http://dx.doi.org/10.1080/10286020.2011.584532

Journal of Asian Natural Products Research
Vol. 13, No. 8, August 2011, 688–699

In-vitro antitumor activity evaluation of hyperforin derivatives

Feng Sun[a†], Jin-Yun Liu[a†], Feng He[a], Zhong Liu[b], Rui Wang[b], Dong-Mei Wang[a], Yi-Fei Wang[b]* and De-Po Yang[a]*

[a]*School of Pharmaceutical Sciences, Sun Yat-Sen University, Guangzhou 510006, China;*
[b]*Biomedicine Research and Development Center, Jinan University, Guangzhou 510632, China*

(*Received 15 January 2011; final version received 25 April 2011*)

The derivatives of hyperforin, namely hyperforin acetate (**2**), 17,18,22,23,27,28,32,33-octahydrohyperforin acetate (**3**), and *N*,*N*-dicyclohexylamine salt of hyperforin (**4**), have been investigated for their antitumor properties. *In-vitro* studies demonstrated that **2** and **4** were active against HeLa (human cervical cancer), A375 (human malignant melanoma), HepG2 (human hepatocellular carcinoma), MCF-7 (human breast cancer), A549 (human nonsmall cell lung cancer), K562 (human chronic myeloid leukemia), and K562/ADR (human adriamycin-resistant K562) cell lines with IC_{50} values in the range of 3.2–64.1 μM. The energy differences between highest occupied molecular orbital and lowest unoccupied molecular orbital of **2**–**4** were calculated to be 0.39778, 0.43106, and 0.30900 a.u., respectively, using the Gaussian 03 software package and *ab initio* method with the HF/6-311 G* basis set. The result indicated that the biological activity of **4** might be the strongest and that of **3** might be the weakest, which was in accordance with their corresponding antiproliferative effects against the tested tumor cell lines. Compound **4** caused cell cycle arrest at G2/M phase in flow cytometry experiment and induced apoptosis by 4′,6-diamidino-2-phenylindole staining and Annexin V-FITC/PI (propidium iodide) double-labeled staining in HepG2 cells. The results indicated a potential for *N*,*N*-dicyclohexylamine salt of hyperforin as a new antitumor drug.

Keywords: hyperforin derivatives; antiproliferative effect; apoptosis; quantum chemistry calculation

1. Introduction

Hyperforin is an abundant nonpolar phloroglucinol derivative isolated from the antidepressant medicinal plant *Hypericum perforatum* L. (St John's wort) and has been widely considered one of the main active components responsible for the antidepressive effect of *H. perforatum* [1]. It showed a wide spectrum of activities such as antidepression [1–3], antibacteria [4,5], anti-inflammation [6,7], and antitumor [8–10]. *In-vitro* and *in-vivo* experiments have evidenced that hyperforin could inhibit the proliferation of various human and rat tumor cells, such as mammary carcinoma MT-450 cells, brain glioblastoma LN229 cells, leukemia K562 and U937 cells, B-cell lymphocytic leukemia cells, and soon [8,11]. Further investigation indicated that hyperforin showed antitumor effects through induction of apoptosis of cancer cells [8,9,11], inhibition of angiogenesis [12,13], suppression of invasion, metastasis [14], and lymphangiogenesis [10].

Hyperforin was reported to cause a dose-dependent generation of apoptotic

*Corresponding authors. Email: lssydp@mail.sysu.edu.cn; twang-yf@163.com
†These authors contributed equally to this research.

ISSN 1028-6020 print/ISSN 1477-2213 online

DOI: 10.1080/10286020.2011.584532
http://www.informaworld.com

oligonucleosomes, typical DNA laddering and apoptosis-specific morphological changes such as homogenization and vacuolization of mitochondria. The loss of mitochondrial transmembrane potential caused the changes in morphology and permeabilization of mitochondria and the release of cytochrome *c* from mitochondria, and thus, caspase-3 and caspase-9 were activated, which triggered a mitochondria-mediated apoptosis pathway [8]. In a proapoptotic study by Quiney *et al.* [9], hyperforin was found to promote apoptosis of B-cell chronic lymphocytic leukemia cells, by disruption of the mitochondrial transmembrane potential, activation of caspase-3, cleavage of the caspase substrate poly ADP-ribose polymerase-1 (PARP-1), induction of downregulation of Bcl-2, Mcl-1, the cell cycle inhibitor p27 (kip1), and the nitric oxide synthase of type 2.

Angiogenesis is a prerequisite for the growth and metastasis of tumor. Hyperforin was demonstrated to inhibit angiogenesis *in-vitro* and *in-vivo*, by inhibiting the growth, invasion, and metastasis of endothelial cells, abrogating capillary tube formation on Matrigel, inhibiting the production and secretion of urokinase, matrix metalloproteinase 2 (MMP-2), and MMP-9, and decreasing the release of vascular endothelial growth factor (VEGF), which are key events in tumor angiogenesis [12,13].

Both hyperforin and aristoforin inhibited lymphangiogenesis by the suppression of lymphatic capillary outgrowth [10]. Hyperforin showed cytotoxicity and inhibition of matrix proteinases, tumor invasion, and metastasis for the following reasons: inhibition of various proteinases such as the leukocyte elastase, cathepsin G, and urokinase-type plasminogen activator in a dose-dependent and noncompetitive manner; inhibition of extracellular signal-regulated kinase 1/2; and reduction of MMP-2 and MMP-9 secretion. Hyperforin also reduced inflammatory infiltration, neovascularization, size of experimental metastases, and number of lung metastases in mice [14].

However, the potential clinical application of hyperforin is limited by its poor stability exposed to light, heat, and oxygen. Several analogs have been synthesized to improve the stability of hyperforin, which retain good antidepressant activity. The hyperforin derivatives 17,18,22,23,27,28,32,33-octahydrohyperforin, aristoforin, and 17,18,22,23,27,28,32,33-octahydroaristoforin inhibited MT-450 cell proliferation and induced apoptosis *in-vitro*. Aristoforin showed a significant inhibitory effect on tumor growth in the MT-450 tumor-bearing animals, whereas 17,18,22,23,27,28,32,33-octahydrohyperforin and 17,18,22,23,27,28,32,33-octahydroaristoforin showed no effect *in-vivo*, suggesting that the double bonds in the isoprene side chains might contribute to the *in-vivo* effect of the derivatives [15].

In this study, three hyperforin derivatives, hyperforin acetate (**2**), 17,18,22,23,27,28,32,33-octahydrohyperforin acetate (**3**), and *N,N*-dicyclohexylamine salt of hyperforin (**4**), were synthesized and subjected to cell-growth inhibition assay against HeLa, A375, HepG2, MCF-7, A549, K562, and K562/ADR cell lines. Compound **4** was shown to be the most effective one, which could arrest cell cycle at the G2/M phase and induce apoptosis in HepG2 cells. Moreover, the quantum chemistry calculations suggested a correlation between the inhibitory activities against tumor cells and the frontier molecular orbital energy differences of these compounds.

2. Results and discussion

2.1 Inhibition of cell growth by hyperforin derivatives

The concentration-growth inhibition rate curves of hyperforin derivatives are shown in Figure 1. Compound **2** showed significant cytotoxic activities against A375 and HepG2 from 1.6 μM and against the other

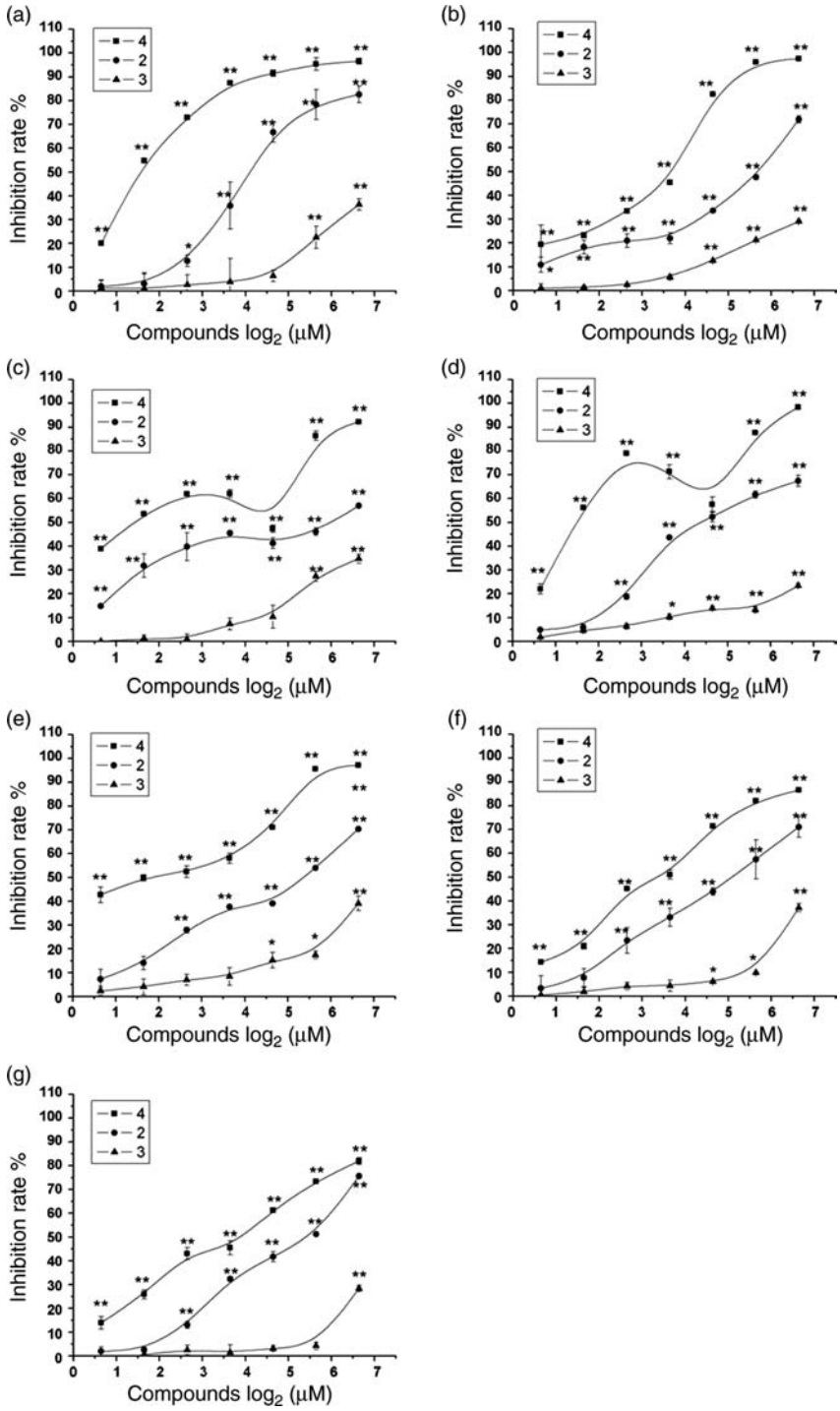

Figure 1. Inhibition rates of cells growth by hyperforin derivatives in (A) HeLa, (B) A375, (C) HepG2, (D) MCF-7, (E) A549, (F) K562, and (G) K562/ADR cell lines (significantly different from the negative control, $*p < 0.05$, $**p < 0.01$).

tumor cell lines from 6.2 μM. The inhibition rates toward the tumor cell lines were in the range from 56.98 to 82.63% at the concentrations of 1.6–100 μM. Compound **4** showed antiproliferative activities against all the tumor cell lines from the lowest concentration, significantly different from the negative control ($p < 0.01$). The inhibition rates were in the range from 81.95 to 98.38% at the concentrations of 1.6–100 μM. Compounds **2** and **4** showed dose-dependent inhibition activities toward HeLa, A375, A549, K562, and K562/ADR cell lines. Interestingly, the inhibition of **2** against HepG2 and **4** against HepG2 and MCF-7 cell lines had a tendency of ascending, descending, and ascending with the increase of the dose. The reason of the result might be that the compounds with different concentration induced the apoptosis of these tumor cells for different reasons, which remains to be further studied.

The half maximal inhibitory concentration (IC_{50}) values of hyperforin derivatives are summarized in Table 1. The data showed that compounds **2** and **4** inhibited the growth of different types of tumor cells with IC_{50} values in the range of 2.7–58.9 μM, whereas compound **3** inhibited the growth of all the cell lines at higher concentrations ($IC_{50} > 100$ μM) compared with compounds **2** and **4**. The result supported the opinion of Gartner that the presence of the double bonds in the isoprene side chains (**2** and **4**) favored the antiproliferative activity [15]. Overall, HepG2 cell line was the most susceptible to compound **4**, followed by the MCF-7 cell line, whereas the HeLa cell line was the most sensitive one by the exposure to compound **2**. Compound **4**, the most active derivative, showed selectivity for HepG2, MCF-7, HeLa, and A549 cell lines. In addition, it showed a good antiproliferative effect against K562/ADR with an IC_{50} value of 14.3 μM, which was much lower than that (66.9 μM) of adriamycin. Compounds **2** and **4** demonstrated excellent antiproliferative activities on various human tumor cell lines from diverse target organs, including leukemia and solid tumors. The results suggested that these compounds had promising antitumor activity against a broad spectrum of human tumors.

2.2 Relationship between frontier molecular orbitals and activities of hyperforin derivatives

In general, the main factors that affect the biological activities of molecules are frontier molecular orbitals including the highest occupied molecular orbital (HOMO) and lowest unoccupied molecular orbital (LUMO). The interaction between the active molecules and their receptors, i.e. biomacromolecules, mainly occurs near the frontier molecular orbitals of both molecules. The HOMO and its vicinal occupied orbitals are prone to donate electrons, whereas the LUMO and its vicinal unoccupied orbitals are prone to

Table 1. *In-vitro* antiproliferative activity against several tumor cells.

	Compounds [IC_{50} (μM)]			
Cell lines	**2**	**3**	**4**	Adriamycin
HeLa	17.3 ± 2.1	>100	3.1 ± 0.1	2.1 ± 0.1
A375	50.6 ± 1.5	>100	12.4 ± 1.3	0.4 ± 0.1
HepG2	58.9 ± 3.3	>100	2.7 ± 0.1	3.0 ± 0.1
MCF-7	21.7 ± 1.8	>100	2.8 ± 0.1	3.1 ± 0.1
A549	41.4 ± 0.3	>100	3.7 ± 1.1	3.1 ± 0.4
K562	34.3 ± 4.1	>100	9.9 ± 0.2	1.0 ± 0.2
K562/ADR	41.6 ± 0.9	>100	14.3 ± 0.4	66.9 ± 4.5

accept electrons. The lower the energy difference between HOMO and LUMO is, the more liable the interaction is to occur [16–18].

The HOMO energies of compounds **2**–**4** were calculated to be −0.26021, −0.29080, and −0.19874 a.u., respectively, and their corresponding LUMO energies were 0.13757, 0.14026, and 0.11026 a.u., respectively. As a result, the energy differences between HOMO and LUMO of these three compounds were calculated to be 0.39778, 0.43106, and 0.30900 a.u., respectively. The results indicated that compound **4** might have the strongest biological activity as it had the least energy difference between HOMO and LUMO, followed by compound **2**, and the activity of compound **3** might be the weakest, which showed reasonable agreement with their corresponding antiproliferative effects against the tested tumor cell lines in this study. As both compounds **2** and **4** have isoprene side chains, as all the double bonds in the isoprene side chains of compound **3** have been hydrogenated, it can be inferred that the double bonds in the isoprene side chains might play a role in chemical regulation of anticancer activity. Compound **2** is an acetate of hyperforin at the C-7 hydroxyl group, whereas compound **4** is a nitrogen salt of hyperforin at the same position, indicating that suitable hydrophilic substituted enolized β-dicarbonyl system might improve the activity.

2.3 Induction of apoptosis by N,N-*dicyclohexylamine salt of hyperforin*

Next, we investigated whether the growth inhibition effects of compound **4** on cells were due to apoptosis by 4′,6-diamidino-2-phenylindole (DAPI) staining and Annexin V-FITC/PI double-labeled flow cytometry analysis.

HepG2 cells were stained with DAPI to observe abnormal cell morphology by laser confocal scanning microscopy. The cell nuclei in the control group without compound **4** treatment emitted uniform blue fluorescence, indicating that the cells were normal and the nuclei were intact, whereas apoptotic bodies that have typical morphological characteristics of apoptosis (Figure 2) appeared after the exposure of the cells to 1, 5, and 40 μM of compound **4** for 48 h. The apoptotic bodies in the group treated with 5 or 40 μM of compound **4** were much more than those in the group treated with 1 μM of compound **4**; whereas the total number of cells in the 40 μM group were much lower than those in the 5 μM group, and more shriveled and deformed cell nuclei were observed in the former, showing a dose-dependent effect.

In addition, Annexin V-FITC/PI double-labeled flow cytometry analysis confirmed the apoptosis induced by compound **4**. HepG2 cells were treated for 48 h with this compound over a concentration range from 1 to 40 μM, and the degree of cell apoptosis was evaluated by Annexin V-FITC/PI double-labeled flow cytometry. Figure 3 shows that little binding with Annexin V-FITC was observed in untreated HepG2 cells. However, after treatment of cells with compound **4** at concentrations of 1, 5, and 40 μM for 48 h, the apoptotic percentage reached 12.6 ± 0.8, 31.6 ± 1.0, and 60.5 ± 2.8%, dose dependently, significantly different from that of the control (3.5 ± 0.6%) ($p < 0.01$). The results combined with the morphological changes indicated that the antiproliferative effect of compound **4** correlated with the induction of apoptosis.

2.4 Cell cycle arrest induced by N,N-*dicyclohexylamine salt of hyperforin*

Propidium iodide (PI) staining analysis was performed on HepG2 cells after treatment with different concentrations of compound **4**, and the cell cycle distribution was analyzed by flow cytometry. The results of cell cycle analysis are presented in Table 2 and Figure 4. The data demonstrated that the percentage of cells

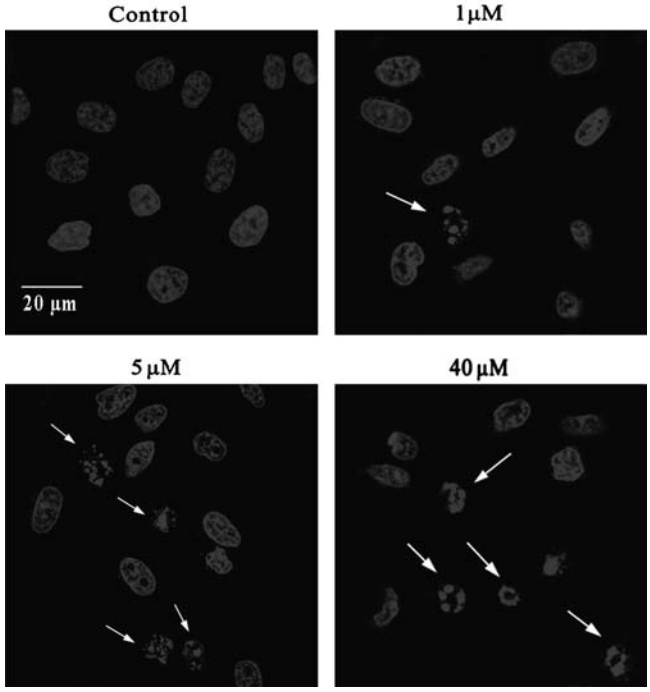

Figure 2. Morphological study of HepG2 cells treated with compound **4** for 48 h by DAPI staining with laser confocal scanning microscopy. The arrows indicate the nuclear fragmentation. Scale bar = 20 μm.

in G1 phase was significantly higher in cell samples incubated with compound **4** at a concentration of 40 μM than that in the control group. And the proportion of G2/M phase cells treated with compound **4** increased remarkably in a dose-dependent manner. However, the proportion of S phase cells had no significant change. The result indicated that compound **4** might induce apoptosis of HepG2 cells mainly by G2/M phase arrest.

3. Conclusions

This study demonstrated that hyperforin acetate and *N*,*N*-dicyclohexylamine salt of hyperforin showed good *in-vitro* antiproliferative activity in a variety of cell lines derived from human hematologic malignancies and solid tumors, such as HeLa, A375, HepG2, MCF-7, A549, K562, and K562/ADR cell lines. The potential clinical applications of hyperforin derivatives in the treatment of various cancers are promising. The results of quantum chemistry calculations showed that compounds **4**, **2**, and **3** might have an anticancer potency in descending order, which was consistent with the results of *in-vitro* antitumor experiments. It is also important to note that *N*,*N*-dicyclohexylamine salt of hyperforin showed the antitumor effect through induction of cell apoptosis and elongating the G2/M phase of the cell cycle. Further studies on a detailed mechanism of apoptosis induced by hyperforin derivatives are currently underway in our laboratory.

4. Experimental

4.1 Material

The hyperforin derivatives were synthesized as described in the literature procedure (shown in Scheme 1) and hyperforin was obtained from the *H. perforatum* extract (containing 5% hyperforin) purchased from Shaanxi Jiahe

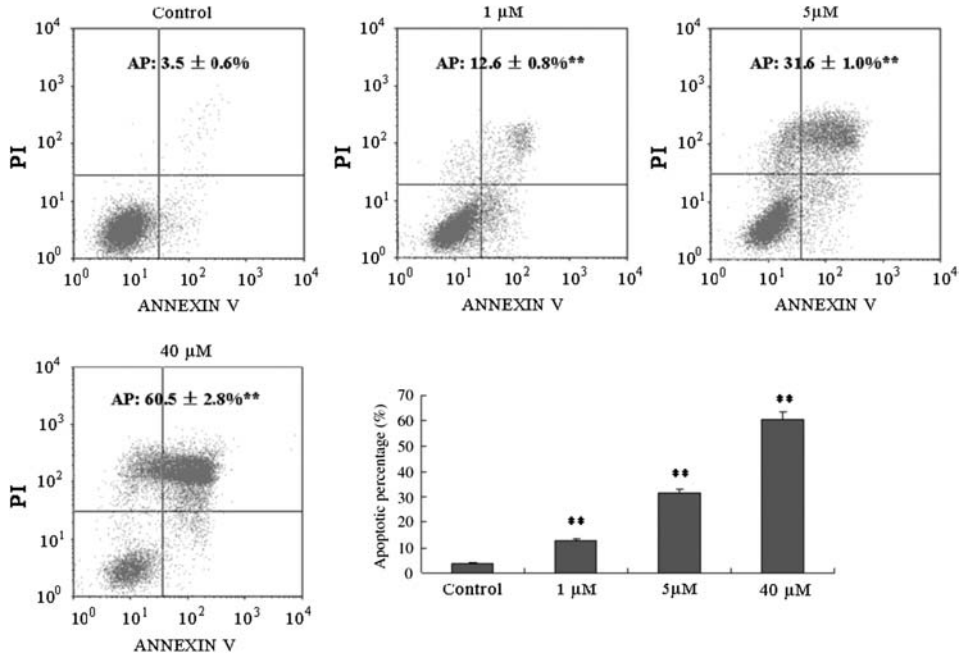

Figure 3. Induction of apoptosis by compound **4** in HepG2 cells. The figures are representative of three separate experiments. Data represent the means ± SD of at least three independent experiments (significantly different from the negative control, $^{**}p < 0.01$).

Phytochem Co. Ltd (Shaanxi, China). Their structures (Figure 5) were identified by comparison with literature values [19–21]. Adriamycin (doxorubicin hydrochloride for injection) was purchased from Zhejiang Hisun Pharmaceutical Co. Ltd (Zhejiang, China).

4.2 Cell culture

K562 cells (ATCC, Manassas, VA, USA) and K562/ADR cells (kindly provided by Prof. Qing-Duan Wang at Academy of Medical and Pharmaceutical Sciences, Zhengzhou University) induced from K562 cell line by adriamycin were grown in RPMI-1640 (Gibco, Paisley, UK) with 10% heat-inactivated fetal bovine serum (FBS) and treated with 100 U/ml penicillin and 100 μg/ml streptomycin. HeLa, A375, HepG2, MCF-7, and A549 cells (offered by Guangzhou Jinan Biomedicine Research and Development Center) were routinely grown in Dulbecco's Modified Eagle Media (DMEM) (Gibco) supplemented with 10% heat-inactivated FBS and treated with 100 U/ml penicillin and 100 μg/ml

Table 2. The effect of compound **4** on the cell cycle of HepG2 cells.

	% HepG2 cells			
Cell cycle phase	Control	1 μM	5 μM	40 μM
G1	63.6 ± 1.2	66.3 ± 1.4	61.7 ± 0.5	55.6 ± 2.5**
S	28.7 ± 0.8	26.8 ± 1.1	27.0 ± 1.3	25.4 ± 2.6
G2/M	7.0 ± 1.3	6.8 ± 1.0	11.2 ± 1.4*	19.0 ± 1.6**

Notes: Data represent the percentage of cells in a particular phase of the cell cycle after 48 h of treatment with compound **4**. Data are representative of three independent experiments (vs. control, $^{*}p < 0.05$, $^{**}p < 0.01$).

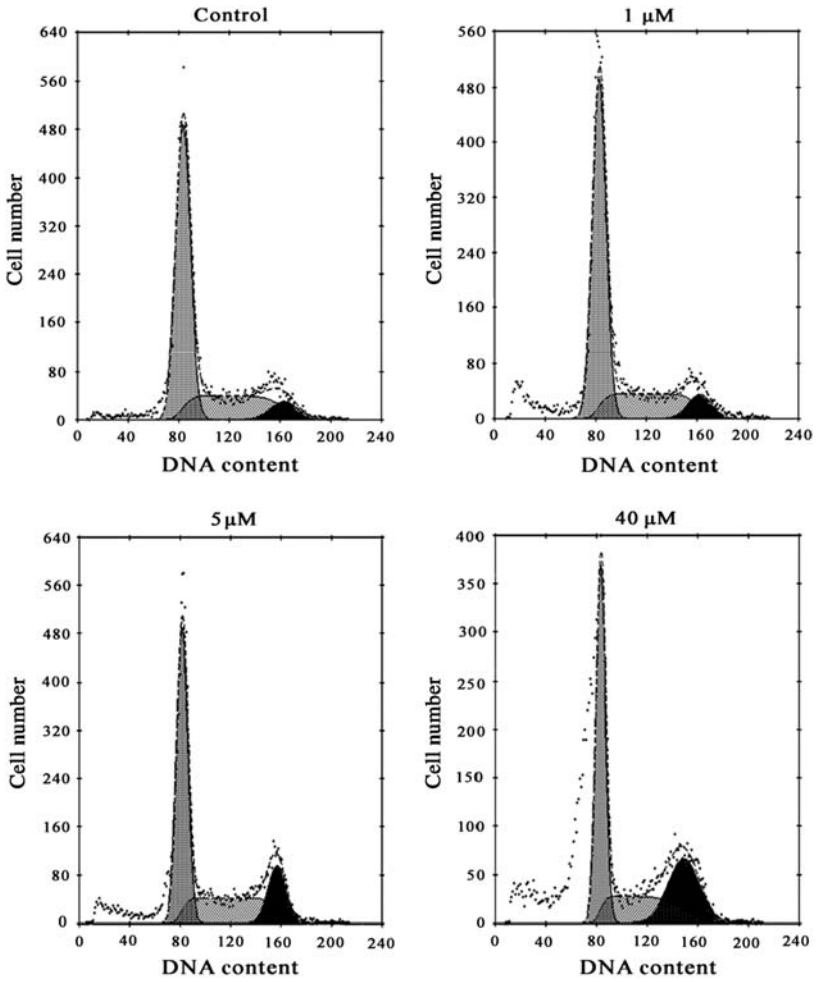

Figure 4. Analysis of cell cycle. Percentages of cells in G1, S, and G2/M phases are presented in histogram. The figures are representative of three separate experiments.

streptomycin. The cells were incubated at 37°C in a humid atmosphere containing 5% CO_2 in air.

4.3 Inhibition of cell proliferation by hyperforin derivatives

To determine the effect of hyperforin derivatives on cell growth, the *in-vitro* cytotoxic activities of compounds **2**–**4** were tested against six tumor cell lines for 48 h by means of the 3-(4,5-dimethylthiaz ol-2-yl)-2,5-diphenyl-2H-tetrazolium bromide (MTT) assay as described by Mossmann [22]. The hyperforin derivatives stock solutions at 50 mM in dimethylsulfoxide (DMSO) were stored at −20°C. Adriamycin was used as positive control. HeLa, A375, HepG2, MCF-7, and A549 cells were plated onto 96-well plates at 1×10^5-cells/well in DMEM with 10% heat-inactivated FBS and incubated for 24 h. Cells were treated with different concentrations of these derivatives in the range of 1.6–100 μM in 96-well plates for 48 h. K562 and K562/ADR cells were plated onto 96-well plates at 2×10^5 cells/well in RPMI-1640 with 10% heat-inactivated

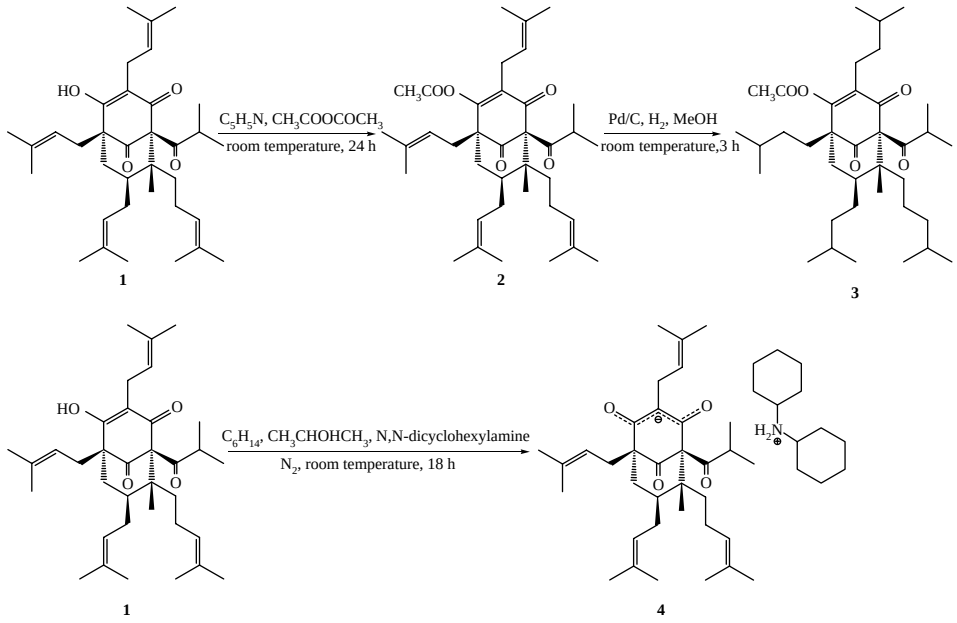

Scheme 1. Reagents and conditions: (a) C_5H_5N, $(CH_3CO)_2O$, RT; (b) MeOH, 5% Pd/C, H_2, RT; and (c) hexane-isopropanol (98:2), *N*,*N*-dicyclohexylamine, RT.

FBS and treated with various concentrations of these derivatives as above for 48 h. Then, 20 μl of RPMI-1640 or DMEM medium with 10% FBS and 5 mg/ml MTT was added. The precipitated formazan was dissolved in 100 μl DMSO. Cell viability was evaluated by optical density reading at 570 nm. Three independent sets of experiments conducted in triplicates were evaluated, and the results were expressed as the percentage reduction in cell viability compared with those of untreated control cultures.

4.4 Quantum chemistry calculations

To investigate the relationship between the molecular structure of hyperforin derivatives and their anitumor activity, the quantum chemical calculation of these compounds was carried out using the Gaussian 03 software package and *ab initio* method with the HF/6-311 G* basis

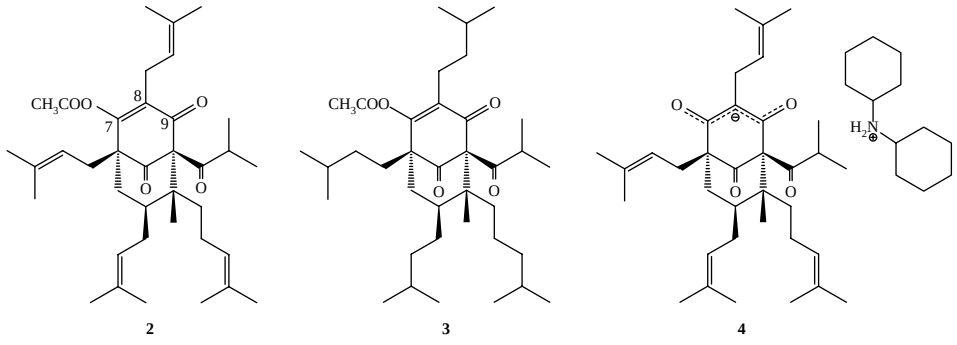

Figure 5. Chemical structures of hyperforin derivatives.

set [23]. The equilibrium molecular geometry configuration and molecular orbital energy level of hyperforin derivatives were determined after optimization calculation. The energy differences between HOMO and LUMO of hyperforin derivatives were combined with their IC_{50} values derived from the MTT assays to discuss the structure–activity relationships.

4.5 Morphological examination of apoptotic cells

Apoptotic morphology was studied by staining the cells with DAPI fluorometric dye. Cells were washed three times with phosphate buffered saline (PBS) after being incubated with 5 μM *N*,*N*-dicyclohexylamine salt of hyperforin for 48 h. Cells were then stained with DAPI for 1 h in the dark. And a laser confocal scanning microscope (LSM 510 META DUO SCAN, Carl Zeiss, Jena, Germany) was used to observe the cell morphology.

4.6 Flow cytometric analysis of apoptosis induced by N,N-dicyclohexylamine salt of hyperforin

In apoptotic cells, the membrane phospholipid phosphatidylserine (PS) is translocated from the inner to the outer leaflet of the plasma membrane, thereby exposed to the external cellular environment. Annexin V is a Ca^{2+}-dependent phospholipid-binding protein with an extremely high affinity for PS. Therefore, the Annexin V-FITC/PI staining was used to determine whether cell viability impacted by *N*,*N*-dicyclohexylamine salt of hyperforin was related to programmed cell death (apoptosis) or necrosis procedure.

HepG2 cells were plated at a density of 1×10^5 cells/well on six-well plates. After treatment with *N*,*N*-dicyclohexylamine salt of hyperforin for 48 h, HepG2 cells were washed with cold PBS, then stained with 100 μl incubation buffer containing Annexin V-FITC/PI, and incubated at 37°C free from light for 15 min. Thereafter, treated cells were immediately analyzed in a FACSCanto II flow cytometer (ELITE, Beckman Coulter, Fullerton, CA, USA). The percentage of apoptotic cells was determined by the MultiCycle software (Phoenix Flow Systems, San Diego, CA, USA). The fluorochrome was excited using the 488-nm light of argon ion laser, and Annexin V and PI emissions were monitored at 525 and 630 nm, respectively. In each analysis, 10,000 events were recorded. The dual parametric dot plots were used for calculation of the percentage of nonapoptotic viable cells in the lower left quadrant (Annexin V-negative/PI-negative), early apoptotic cells in the lower right quadrant (Annexin V-positive/PI-negative), late apoptotic or necrotic cells in the upper right quadrant (Annexin V-positive/PI-positive), and mechanically injured cells in the upper left quadrant (Annexin V-negative/PI-positive).

4.7 Analysis of cell cycle distribution after treatment with N,N-dicyclohexylamine salt of hyperforin

HepG2 cells were plated at a density of 1×10^5 cells/well on six-well plates. After treatment with *N*,*N*-dicyclohexylamine salt of hyperforin for 48 h, the cells were washed three times with PBS. An equal volume of ethanol was added to the cells and kept overnight at 4°C. The cells were washed twice and resuspended in PBS. Then, 100 μg/ml RNase was added and incubated with cells for 1 h at 37°C. PI was added at a final concentration of 0.05 mg/ml followed by 0.5 h incubation protected from light. DNA content was analyzed using a FACSCanto II flow cytometer (ELITE, Beckman Coulter). Data analysis was carried out using WINMDI 2.9 Version (Phoenix Flow Systems).

4.8 Statistical analysis

The data presented are expressed as the means ± SD of three independent experiments. Statistical significance was

estimated by one-way analysis of variance followed by Dunnett's test for unpaired observations, with significance at $p < 0.05$.

Acknowledgements

This work was supported by the Australia–China Special Fund for Scientific and Technological Cooperation (30470188), International Science and Technology Cooperation Program of China (2009DF31230), External Cooperation of Science and Technology of Guangdong Province, China (2009B050500002), Guangdong Natural Science Foundation (1045100 8901004959), China Postdoctoral Science Foundation (20090450194), and the Fundamental Research Funds for the Central Universities (21609303).

References

[1] S.S. Chatterjee, S.K. Bhattacharya, M. Wonnemann, A. Singer, and W.E. Müller, *Life Sci.* **63**, 499 (1998).

[2] W.E. Muller, A. Singer, M. Wonnemann, U. Hafner, M. Rolli, and C. Schafer, *Pharmacopsychiatry* **31**, 16 (1998).

[3] A. Singer, M. Wonnemann, and W.E. Müller, *J. Pharmacol. Exp. Ther.* **290**, 1363 (1999).

[4] P. Avato, F. Raffo, G. Guglielmi, C. Vitali, and A. Rosato, *Phytother. Res.* **18**, 230 (2004).

[5] C. Cecchini, A. Cresci, M.M. Coman, M. Ricciutelli, G. Sagratini, S. Vittori, D. Lucarini, and F. Maggi, *Planta Med.* **73**, 564 (2007).

[6] K.D.P. Hammer, M.L. Hillwig, A.K.S. Solco, P.M. Dixon, K. Delate, P.A. Murphy, E.S. Wurtele, and D.F. Birt, *J. Agric. Food Chem.* **55**, 7323 (2007).

[7] C. Feisst, C. Pergola, M. Rakonjac, A. Rossi, A. Koeberle, G. Dodt, M. Hoffmann, C. Hoernig, L. Fischer, D. Steinhilber, L. Franke, G. Schneider, O. Radmark, L. Sautebin, and O. Werz, *Cell. Mol. Life Sci.* **66**, 2759 (2009).

[8] C.M. Schempp, V. Kirkin, B. Simon-Haarhaus, A. Kersten, J. Kiss, C.C. Termeer, B. Gilb, T. Kaufmann, C. Borner, J.P. Sleeman, and J.C. Simon, *Oncogene* **21**, 1242 (2002).

[9] C. Quiney, C. Billard, A.M. Faussat, C. Salanoubat, A. Ensaf, Y. Nait-Si, J. Fourneron, and J.P. Kolb, *Leukemia* **20**, 491 (2006).

[10] M. Rothley, A. Schmid, W. Thiele, V. Schacht, D. Plaumann, M. Gartner, A. Yektaoglu, F. Bruyere, A. Noel, A. Giannis, and J.P. Sleeman, *Int. J. Cancer* **125**, 34 (2009).

[11] K. Hostanska, J. Reichling, S. Bommer, M. Weber, and R. Saller, *Eur. J. Pharm. Biopharm.* **56**, 121 (2003).

[12] B. Martinez-Poveda, A.R. Quesada, and M.A. Medina, *Int. J. Cancer* **117**, 775 (2005).

[13] C. Quiney, C. Billard, P. Mirshahi, J.D. Fourneron, and J.P. Kolb, *Leukemia* **20**, 583 (2006).

[14] M. Dona, I. Dell'Aica, E. Pezzato, L. Sartor, F. Calabrese, M. Della Barbera, A. Donella-Deana, G. Appendino, A. Borsarini, R. Caniato, and S. Garbisa, *Cancer Res.* **64**, 6225 (2004).

[15] M. Gartner, T. Muller, J.C. Simon, A. Giannis, and J.P. Sleeman, *Chembiochem* **6**, 171 (2005).

[16] W.G. Richards, *Quantum Pharmacology* (Butterworths, London, 1983), p. 153.

[17] B.P. Bandgar, S.S. Gawande, R.G. Bodade, J.V. Totre, and C.N. Khobragade, *Bioorg. Med. Chem.* **18**, 1364 (2010).

[18] A.K. Bhattacharjee, J.A. Gordon, E. Marek, A. Campbell, and R.K. Gordon, *Bioorg. Med. Chem.* **17**, 3999 (2009).

[19] L. Verotta, G. Appendino, E. Belloro, F. Bianchi, O. Sterner, M. Lovati, and E. Bombardelli, *J. Nat. Prod.* **65**, 433 (2002).

[20] E. Bombardelli, P. Marazzoni, A. Riva, N. WO 03091194 (A1) Fuzzati, (2003).

[21] S.S. Chatterjee, C. Erdelmeier, K. Klessing, D. Marme, C. WO 9941220 Schachtele, (1999).

[22] T. Mosmann, *J. Immunol. Methods* **65**, 55 (1983).

[23] M.J. Frisch, G.W. Trucks, H.B. Schlegel, G.E. Scuseria, M.A. Robb, J.R. Cheeseman, J.A. Montgomery, T. Vreven Jr, K.N. Kudin, J.C. Burant, J.M. Millam, S.S. Iyengar, J. Tomasi, V. Barone, B. Mennucci, M. Cossi, G. Scalmani, N. Rega, G.A. Petersson, H. Nakatsuji, M. Hada, M. Ehara, K. Toyota, R. Fukuda, J. Hasegawa, M. Ishida, T. Nakajima, Y. Honda, O. Kitao, H. Nakai, M. Klene, X. Li, J.E. Knox, H.P. Hratchian, J.B. Cross, V. Bakken, C. Adamo, J. Jaramillo, R. Gomperts, R.E. Stratmann, O. Yazyev, A.J. Austin, R. Cammi, C. Pomelli, J.W. Ochterski, P.Y. Ayala, K. Morokuma,

G.A. Voth, P. Salvador, J.J. Dannenberg, V.G. Zakrzewski, S. Dapprich, A.D. Daniels, M.C. Strain, O. Farkas, D.K. Malick, A.D. Rabuck, K. Raghavachari, J.B. Foresman, J.V. Ortiz, Q. Cui, A.G. Baboul, S. Clifford, J. Cioslowski, B.B. Stefanov, G. Liu, A. Liashenko, P. Piskorz, I. Komaromi, R.L. Martin, D.J. Fox, T. Keith, M.A. Al-Laham, C.Y. Peng, A. Nanayakkara, M. Challacombe, P.M.W. Gill, B. Johnson, W. Chen, M.W. Wong, C. Gonzalez, and J.A. Pople, *Gaussian 03, Revision D.1* (Gaussian, Inc, Wallingford, CT, 2005).